Reactive and Functional Polymers 226 (2026) 106827

Contents lists available at ScienceDirect

Reactive and Functional Polymers

journal homepage: www.elsevier.com/locate/react

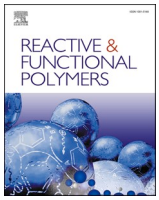

The effects of molecular fortification on the compression and shear properties of a commercial epoxy resin system

Bohao Zhang [a], Rachel Board [a], Eleni Georgiou [a], Laurie-Anne Entzmann [a], Joe Rifai [a], Nicolas S.T. Darras [a], Matthew Bone [a], Gustavo Quino [b], Milo S.P. Shaffer [c], Ian Hamerton [a,*]

[a] Bristol Composites Institute, School of Civil, Aerospace, and Design Engineering, University of Bristol, Queen's Building, University Walk, Bristol BS8 1TR, UK
[b] Department of Aeronautics, Imperial College London, South Kensington Campus, London SW7 2AZ, UK
[c] Department of Chemistry, Imperial College London, South Kensington Campus, London SW7 2AZ, UK

ARTICLE INFO

Keywords:
Molecular fortifiers
Epoxy resins
Molecular modelling
Compression
Shear

ABSTRACT

This study seeks to determine the viability of molecular fortification of a commercially available epoxy system based on the RS-M135 epoxy with the RS-MH137 hardener. Four possible fortifiers, dimethyl carbonate (DMC), dimethyl sulfoxide (DMSO), bis(4-hydroxyphenyl)phenylphosphine oxide (BHPPO), and 9,10-dihydro-9-oxa-10-phosphaphenanthrene-10-oxide (DOPO) were studied. DMC and DMSO have previously been used as fortifiers while BHPPO and DOPO were selected due to their reduced toxicity compared with dimethyl methyl phosphonate (DMMP). Mechanical properties of the fortified resins are investigated in compression and shear. Significant increases in the compression properties (11% increase in compression modulus and 24% in peak yield stress with 2 mol% DMSO) and the shear properties (16% increase in shear modulus and 15% in peak yield stress with 4 mol% DMSO) respectively are observed following fortification with DMSO. The improvement in the compressive properties (13% increase in compression modulus and 13% in peak yield stress with 2 mol% DMC) is also observed in the blends containing DMC, although to a lesser degree. Differential scanning calorimetry analysis reveals that there is evidence of modest levels of co-reaction and a very slight drop in the glass transition temperature on addition of the fortifiers (*i.e.* a reduction of up to 3 °C in the case of DMSO and 8 °C in the case of DMC, when 16 mol% of either fortifier was added), while thermogravimetric analysis confirms that the onset of thermal degradation is practically unchanged. Molecular dynamics modelling confirms the compatibility of DMSO and DMC with the epoxy blend but indicates that the BHPPO and DOPO undergo strong self-association, reducing their ability to be dispersed effectively within the epoxy blend.

1. Introduction

Fibre-reinforced polymer composites are the current state-of-the-art for lightweight structures and their use is rising exponentially in a wide range of applications from aerospace to sporting goods. However, the present challenge is to improve the absolute performance of composites in compression, through the approach of quantitative hierarchical design. In composites, attention often focusses on the high strength and stiffness of the primary reinforcing fibres and may overlook the resin matrix that holds them together. However, the matrix typically accounts for around half the total composite volume and may play an important role in determining the performance in compression. The challenge is to improve the stress and stiffness of the resin, particularly as it shears between the fibres, without reducing the toughness of the composite.

The use of nonreactive or noncovalently bound fortifiers has been observed to reinforce the network of the polymer matrix at a molecular scale to improve the mechanical properties of a highly crosslinked network [1,2]. These molecular fortifiers are a group of compounds that have displayed the ability to increase *e.g.* yield stress and modulus [3,4]. This is the converse effect of the group of additives known as plasticisers, however examples of both plasticisers and fortifiers have been observed to reduce the measured glass transition temperature (T_g) of polymers including epoxy resins [5,6]. Molecular fortification is particularly applicable to polymers with stiff polar groups and rigid chains as exemplified by bisphenol A polycarbonates [7]. The process whereby fortification occurs as a result of the added molecules filling free volume [4,8] or displaying specific interactions with the polymer matrix, characterised by the effects on the sub-ambient β-transition [8–10]. For

* Corresponding author.
E-mail address: ian.hamerton@bristol.ac.uk (I. Hamerton).

https://doi.org/10.1016/j.reactfunctpolym.2026.106827
Received 13 December 2025; Received in revised form 15 May 2026; Accepted 28 May 2026
Available online 30 May 2026
1381-5148/© 2026 The Authors. Published by Elsevier B.V. This is an open access article under the CC BY license (http://creativecommons.org/licenses/by/4.0/).

example, Saraf et al. applied dimethyl methylphosphonate (DMMP) into the diglycidyl ether of bisphenol A (DGEBA)- and the diepoxide of bis-hydroxydeoxybenzoin (BEDB)-based resin systems and reported that the elastic modulus was improve by 50% with increasing the concentration of the fortifier [4]. By employing a molecular fortifier formed by the reaction between phenyl glycidyl ether and 2-(acetylamino)phenol, Daly et al. demonstrated that the tensile modulus and strength of a crosslinked epoxy network was improved by suppressing the β-transition [9]. In that study, it was reported that under tension, the network exhibited increased ductility as well as higher overall strength (the tensile strength was increased by 50%, while the shear modulus was increased by 61%).

There have been multiple approaches to determine the ideal fortification molecules: initially it was hypothesised that an aromatic component of the molecule was required and, although they have been used as fortifiers [11], other studies have showed that aliphatic compounds had similar effects on the properties and occasionally even to a greater extent [2]. Several oligomeric compounds were determined to fortify the matrix (a high T_g epoxy resin based on *bis*(2,7 diglycidyl ether naphthalenediol) methane and 4,4′-diaminodiphenylsulfone), however, the most significant improvements in molecular fortification have been observed using low molecular weight compounds with a highly polar functionality.

The inspiration for this study, and the selection of DMC and DMSO, was the work of Lesser et al. [1], who demonstrated using dimethyl methyl phosphonate (DMMP), and dimethyl phosphoramidate which both contain P═O moieties; in this case the hydrogen bond forms with the hydroxyl group that is created in the opening of the epoxide in the formation of the networks and fill free space increasing the physical density of the epoxy. It is well known [12] that the P═O moiety is a particularly strong hydrogen bond base and indeed the DMMP molecule is a recognised nerve agent mimic [10], and so it was decided to seek an alternative for DMMP which presents challenges in use in the engineering laboratory. For this reason, the more readily available commercial flame retardants, bis(4-hydroxyphenyl)phenylphosphine oxide (BHPPO) and 9,10-dihydro-9-oxa-10-phosphaphenanthrene-10-oxide (DOPO) were selected for this study. Properties such as density, viscosity, T_g, and tensile properties are most commonly measured when evaluating the performance of fortified polymers such as epoxy resins [1,5], but the authors are aware of very little publications evaluating the compressive [4] and shear performance of fortified epoxy systems, and this forms the basis of the current study.

Although this previous study reported promising properties in flexure which suggested this material as a potential candidate for this study as the authors are aware of very few publications evaluating the compressive and shear performance of fortified epoxy systems, which forms the basis of the current study.

2. Materials and methods

2.1. Materials

Component A, RS-M135 (PRF Composites, UK) is an epoxy resin produced from bisphenol A diglycidyl ether (DGEBA, 1) (CAS No. 25068–38-6) with a number average molecular weight, Mn < 700 g/mol. (70–90% *w*/w) and containing an added proportion of 1,6-hexanediol diglycidyl ether (DEGH, 2) (CAS No. 16096–31-4) as a reactive diluent. Component B, RS-MH137 (PRF Composites, UK), is a curing agent that contains (a) 3-aminomethyl-3,5,5-trimethylcyclohexylamine, 3 (or isophorodiamine, IPDA) (CAS No. 2855-13-2) 35–50% *w*/w, and (b) polyoxypropylenediamine, 4 (CAS No. 9046-10-0) (denoted POPD) 50–70% w/w. The following fortifiers were considered: dimethyl sulfoxide (DMSO) (CAS No. 67–68-5), dimethyl carbonate (DMC) (CAS No. 616–38-6), bis(4-hydroxyphenyl)phenylphosphine oxide (BHPPO) (CAS No. 795–43-7), and 9,10-dihydro-9-oxa-10-phosphahenanthrene-10-oxide (DOPO) (CAS No. 35948–25-5) which were purchased from Sigma Aldrich. The structures of the epoxy components and the molecular fortifiers are shown in Table 1.

2.2. Preparation of fortified materials

2.2.1. Mixing process for the DMSO-fortified epoxy

A series of blends was prepared to determine the ideal concentration of each fortifier by adding the desired amount of DMSO (2, 4, 8, and 16 mol% with respect to the epoxy content). This increment by a factor of 2 was derived from a previous study on DOPO [2]. The DMSO was added to the beaker containing the epoxy resin RS-M135 and manual stirring was performed until the DMSO was entirely mixed within the epoxy. The RS-MH137 curing agent was added according to the specified ratio for the composition and the mixture was then degassed for 20 min at room temperature. The degassed mixture was then poured into a silicone mould and allowed to cure approximately 10 h at room temperature.

2.2.2. Mixing process for the DMC-fortified epoxy

A similar approach was taken to the DMSO blends, but the corresponding volume of DMC was first extracted from the bottle under air-free conditions (the density of the DMC is 1.069 g/cm^3) as the reagent is a highly flammable liquid. Simultaneously, the resin RS-M135 and hardener RS-MH137 were mixed in a flask, in accordance with the ratio, and stirred magnetically. Then oxygen was extracted from the flask, which then filled with nitrogen. Using a nitrogen balloon and syringe, the DMC was added to the mixture and mixed for 5 to 10 min. Then, the mixture was degassed at room temperature using a vacuum pump for 30 min before the degassed mixture was poured into a silicone mould (see Supplementary Material).

2.2.3. Mixing process for the BHPPO-fortified epoxy

The desired amount of BHPPO (2, 4, 8, and 16 mol% with respect to the epoxy) was added to the beaker containing the epoxy resin RS-M135 and stirring was performed (first manually then with slow magnet stirring to avoid introducing to much air) but the fortifier repeatedly formed aggregates at all levels of addition and so it was decided to discontinue experimental work with this compound.

2.2.4. Mixing process for the DOPO-fortified epoxy

The desired amount of DOPO (2, 4, 8, and 16 mol% with respect to the epoxy) was added to the beaker containing the epoxy resin RS-M135 and stirring was performed (first manually then with slow magnet stirring to avoid introducing to much air) but the fortifier repeatedly formed aggregates at all levels of addition and so it was decided to discontinue experimental work with this compound.

2.3. Instrumentation and test methods

2.3.1. Differential scanning calorimetry (DSC)

DSC experiments were performed using a TA DSC Q2000. Hermetically sealed Tzero aluminium pans were used, with sample masses of 10.0 ± 1.0 mg (uncured samples) and 6.1 ± 0.2 mg (cured samples). Samples were equilibrated at 30 °C and then heated to 250 °C at a heating rate of 10 °C/min, unless otherwise stated, with the sample cell kept under a constant nitrogen flow of 50 cm^3/min. Residual curing exotherms were identified by heat/cool/heat scans, using a cooling rate of 10 °C/min, from which the glass transition temperature was determined using the midpoint of the discontinuity in the heat flow *versus* temperature plot. Moreover, the polymerisation enthalpy of the baseline and fortifier-added specimens were determined from the temperature range of 90 °C – 250 °C using a linear baseline.

2.3.2. Simultaneous thermal analysis (STA)

STA measurements were performed using a Netzsch STA 449 F3 Jupiter instrument equipped with alumina sample pans. Experiments were undertaken on cured samples with masses of 8.5 ± 0.3 mg in a N_2

Table 1
Chemical structures of the components in the commercial epoxy resin and the molecular fortifiers.

RS-M135			
Compound			Structure
Bisphenol A diglycidyl ether (shown as dimer)			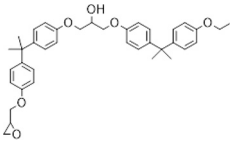
1,6-bis(2,3-epoxypropoxy)hexane			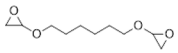
RS-MH137 Poly(oxypropylene) diamine			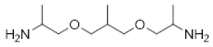
3-aminomethyl-3,5,5-trimethylcyclohexylamine			
Molecular fortifier	Molecular weight g/mol	Boiling point ^{0}C	Structure
Dimethyl sulfoxide (DMSO)	78.13	189	
Dimethyl carbonate (DMC)	90.08	90	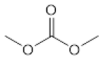
Bis(4-hydroxyphenyl) phenylphosphine oxide (BHPPO)	310.3	280	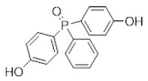
9,10-dihydro-9-oxa-10-phosphahenanthrene-10-oxide (DOPO)	216.17	–	

environment at a heating rate of 10 °C/min. Samples were equilibrated at 30 °C for 10 min and then heated to 800 °C at 10 °C/min. Thermogravimetric analysis (TGA) results of the samples with DMC and DMSO fortifiers were derived from the STA measurements.

2.3.3. X-ray computed tomography

Prior to performing shear testing the machined samples were scanned using X-ray micro-CT to measure the wall thickness of the specimens and to ensure there were no defects (voids or cracks) or variability in the wall thickness in the samples which would impact the repeatability of the test results. A Nikon XTH 320 scanner was used with a voltage of 80 kV and the current used was 86 A with a voxel size of 200 μm.

2.3.4. Compression testing

The samples for compression testing were machined into cylindrical specimens with a 1:1 ratio of length to diameter aspect ratio using a diameter of 6.0 ± 0.1 mm (Fig. 1). These specimens were then spray painted individually using an acrylic mated white spray paint once this had dried black halo speckles with an approximate speckle size of 100 μm were applied over the entire surface of each sample. This pattern was achieved by spraying with an airbrush with commercially available India Ink. These samples were left to dry fully before testing in compression.

Testing was carried out on the Shimadzu test frame AGS 10 kN XD according to the test method developed by Quino et al. [13]. Fig. 2 shows the test setup. A pair of stainless-steel cylindrical compression plates each with diameter of 30 mm with a load cell of 10 kN were used. Each specimen was tested up to the limit of the calibrated load cell that is 9.9 kN. The top and bottom plates were covered with a polytetrafluoroethylene (PTFE) film to reduce friction between the upper and lower surfaces of the cylindrical test specimens with which they come into direct contact. These tapes were replaced between each test. This was used to eliminate any undesirable friction induced deformations

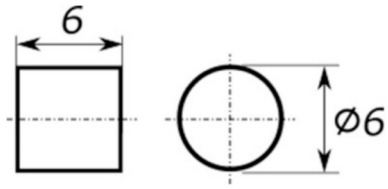

Fig. 1. Dimensions of the compression specimens (mm) [13].

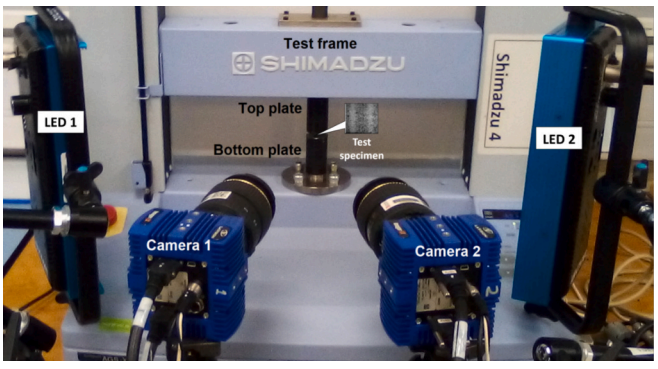

Fig. 2. Compression and digital image correlation (DIC) experimental set-up showing position of compression test specimen (shown in expanded image).

that can occur this includes barrelling of the specimens. The tests were performed at room temperature with a constant vertical displacement rate of 0.36 mm/min. This corresponded to a nominal strain rate in compression of 0.001 s^{-1}. Greyscale images of the speckled specimens were captured, at a frequency of 1 Hz, by a pair of DaVis LaVision 16 MP CMOS stereo Digital Image Correlation (DIC) cameras, positioned symmetrically at an angle of 12° to the test specimen. After calibration and acquisition, images were analysed *via* the DaVis10 LaVision DIC software and synchronised with the load (F) analogue ±5 V output of the Shimadzu universal test frame. The compression test specimens were illuminated by a pair of light-emitting diode (LED) light arrays, throughout the entire duration of the tests. Strain was calculated at the sampling rate of 1 Hz. Five specimens were tested per material system.

2.3.5. Shear testing

The samples for shear testing were cast into cylindrical specimens machined with a 'waisted' configuration with a nominal gauge section of 2.0 mm in length and constant nominal wall thickness of 0.5 mm (Fig. 3), similar to the specimens produced in [14]. These specimens were bonded with two sanded, aluminium endcaps using Scotch-Weld DP490 structural adhesive from 3 M. The curing cycle for the glue was 24 h at room temperature then post-cured for 1 h at 80 °C. The specimens were then spray painted individually using an acrylic mated white spray paint. Once this had dried black halo speckles with an approximate speckle size of 100 μm were applied over the entire gauge section surface of each sample using an airbrush with commercially available India Ink. These samples were left to dry fully.

The shear test was carried out on samples in pure shear using an Instron ElectroPuls E10000 machine (Fig. 4) fitted with a 10 kN axial load and a 100 Nm torque loadcells. The tests were performed at room temperature. Specimens were firstly preloaded with a compressive force of 5 N in 5 s to ensure complete contact with test fixture, followed by shearing at a constant rotation speed of 0.1°/s until failure. The corresponding shear strain rate was 0.0017 s^{-1}. 16 M-pixel complementary metal-oxide-semiconductor (CMOS) stereo DIC cameras, with a pair of external LED light arrays, were used to capture greyscale images of the speckled specimens at a frequency of 1 Hz. The captured images were then processed in the DaVis10 LaVision DIC software. Five specimens were tested per material system.

2.4. Data reduction

During the compression experiment, strains and stresses reported and discussed in this manuscript are engineering strains (ε) and stresses (σ). The strains were obtained *via* DIC analysis and a representative virtual strain gauge (0.5 mm × 0.5 mm), placed at the centre of the generated strain map in specimen gauge section, provided the values for instantaneous engineering axial strain values. The values for axial stress were plotted against the axial strain values and the resulting stress-strain curves were used to determine the compression modulus (E) as the slope from the linear portion of the elastic region of the curve. The peak yield point was defined in the standard ASTM D695 [15] as the point on the curve where stress values stop increasing with increasing strain values. At that point, peak yield stress (σ_y) and peak yield strain (ε_y) were determined for each of the four tested epoxy matrices.

During the shear experiment, the torque (T), and the shear strain (γ) were extracted from the torque loadcell and the DIC software respectively. The shear stress (τ) was calculated from:

$$\tau = \frac{T}{2\pi\bar{r}^2 t} \tag{1}$$

where $\bar{r}$ is the mean radius of the gauge region and t is the wall thickness.

The shear modulus (G) was the slope of the shear stress-strain plot for the shear strain range of 1% and 3%.

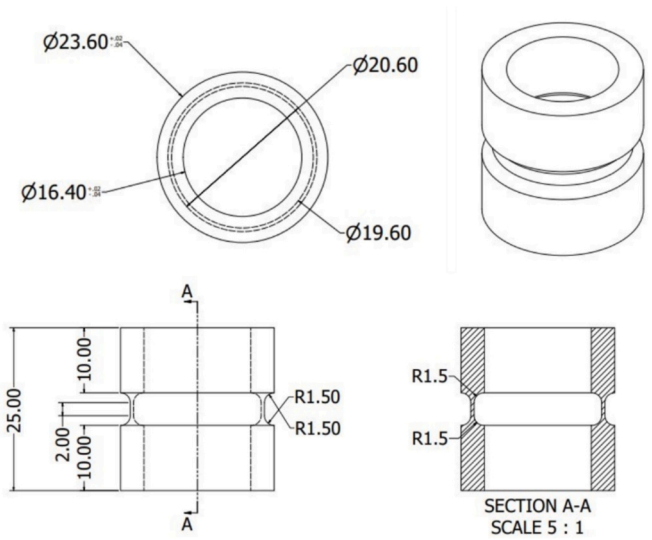

Fig. 3. Dimensions of the shear specimens (mm) [14].

2.5. Modelling methods

Atlas molecular modelling software (Molydyn Ltd., Bristol) was used to simulate models of the epoxy system with the added fortifiers. The DREIDING forcefield, which uses a 12–6 Lennard-Jones potential to describe van der Waals interactions, used to generate the models [16] and the data obtained were visualised in Ovito v. 3.8.4 (Ovito GmbH, Germany). The formulation of epoxy networks was simulated comprising 20,000 atoms in the periodic unit cell built with initial dimensions of 100 Å. The number of epoxy molecules and hardener molecules in the simulation was calculated using the manufacturer's recommended mixture ratio with the molecular weights provided for the molecules in proportions outlined in the manufacturer's data sheet. The molecules were constructed *in silico* and the reaction sites of each molecule were highlighted and numbered. The bonds at each of the reaction sites were then opened and the bonded hardener and epoxy connections were made and the energy was minimised. Each fortifier molecule was added as a non-reactive spectator molecule over a range of compositions and each run within its own simulation. Simulated structures were produced through a standard geometry optimisation, followed by fixed duration canonical and isothermal-isobaric ensemble simulations [17].

3. Results and discussion

3.1. Studying the effects of molecular fortification

3.1.1. Reaction of fortifier addition

During blending, each fortifier was introduced into the epoxy mixture based on partially reacted bisphenol A diglycidyl ether (M_n < 700 g/mol.) and 1,6-hexanediol diglycidyl ether. The driving force for the mixing of the blends is determined predominantly by the affinity of the more polar elements of this mixture (*e.g.* the hydroxyl group of the hydroxypropyl bridge) for the carbonyl or sulphoxide bridging groups, but it is assumed that a small degree of co-reaction of these centres will take place with the epoxy. There is some evidence in the literature that at such low concentrations dimethyl carbonate may participate in a transesterification reaction with the hydroxyl groups present in epoxy resin oligomers (such as DGEBA). At higher DMC concentrations this would serve to introduce polycarbonate linkages [18]. However, at the significantly lower temperatures employed here and with an effective excess of the nucleophile, perhaps more likely is the reaction of DMC with the RS-MH137 diamine hardener *via* non-selective

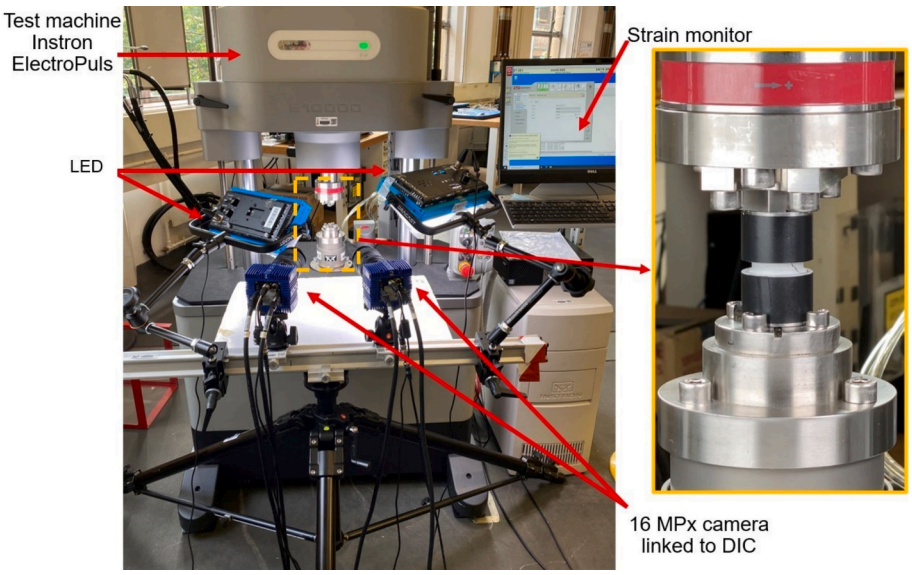

Fig. 4. Experimental setup used for the shear testing (the sample is shown in the expanded image on the right).

carboxymethylation and *N*-methylation reactions [19]. Similarly, the acid-catalysed oxidative ring-opening of epoxides by DMSO is known as a synthetic process that converts epoxides into α-hydroxyketols, this transformation typically requires harsh conditions and proceeds *via* an activated epoxide, which is then attacked by DMSO to yield a stable-functionalized carbonyl product. However, as higher temperatures (*e.g.*, >120 °C), DMSO can take part in the oxidative ring-opening of epoxides or act as an oxygen donor [20]. At the comparatively low concentrations employed in this study, there is some evidence of limited reaction with the epoxy network, as evidenced by the DSC thermograms (Fig. 5, Figs. S1 and S2 for the full dataset). The polymerisation enthalpy, of the base RS-M135/RS-MH137 epoxy was 37.33 J/g, while for the addition of the DMC, the corresponding polymerisation enthalpies were: 2 mol% (39.47 J/g), 4 mol% (30.59 J/g), 8 mol% (21.62 J/g), and 16 mol% (14.71 J/g). While the differences are not large and initially fall within experimental error of the calorimeter, the data indicate that the enthalpy appears to fall with increasing DMC content. Similarly, for the addition of the DMSO, the corresponding polymerisation enthalpies were: 2 mol% (32.96 J/g), 4 mol% (29.35 J/g), 8 mol% (21.1 J/g), and 16 mol% (16.42 J/g). Consequently, it is inferred that even at relatively low levels of reaction, the temperature at the site is locally elevated, and a subsequent reaction is accelerated, resulting in ring opening of the epoxy which still serves to tether the fortifier molecules within the network. All the systems formed dense, well-formed cured products with no visible evidence of macroscopic phase segregation.

3.1.2. *Compression testing*

The compression data for epoxy specimens containing different concentrations of DMC and DMSO are presented in Table 2 (averaged over five specimens). The baseline system (the RS-M135/RS-MH137 epoxy resin) showed an average elastic modulus of 3.1 ± 0.1 GPa, peak yield stress of −71.2 ± 1.5 MPa and peak yield strain of −0.003 ± 0.001. This compares with the data sheet for the same system which states a modulus of 3.3–3.5 GPa [21]. Following the addition of DMC and DMSO, the specimens showed generally higher elastic modulus, peak yield stress and strain. However, the elastic modulus and peak yield stress reduce with increasing the fortifier content from 2 mol% to 16 mol %. No significant variation in peak yield strain is captured.

Blends fortified with either additive displayed similar behaviour in compression (see Fig. S3) and Fig. 6 shows the typical engineering compressive stress *vs.* engineering axial strain curves for the RS-M135/RS-MH137 epoxy fortified with DMC and DMSO (both 16 mol%). Both strains and stresses are compressive and are thus represented by negative values; the initial part of the plot is linear and similar for all the fortified samples. With increasing axial strain, the material yields with a progressive reduction of the tangent modulus, followed by a peak yield stress; the magnitude of the latter falls as the concentration of DMC and DMSO in the blend increases (see Fig. S3).

After this peak yield stress, at strain, the softening regime commences, with a continuous reduction in the compressive stress until strain, possibly driven by the restructuring of molecular chains, represented by the β-transition. This typical behaviour has also been reported in the literature for other epoxy resins [22,23]. The addition of molecular fortifiers is designed to interfere with this restructuring and there is significant variation in the behaviour of the blends. However, barrelling was observed in both representative specimens after peak yield stress for both representative specimens, as indicated in the inserted DIC images. (Owing to the speckling quality of the DMC specimen, full-field strain did not map across the entire gauge section, but it still captured the progression and uniformity of strain during the test.) The final regime in the strain *vs.* stress curve represents strain hardening, where compressive stress increases with strain, mainly driven by the resistance to chain alignment [24–26]. None of the specimens fractured in the experiments although the response becomes increasingly irregular beyond compressive strains of 0.4. The general observed trend is that the addition of 2 or 4 mol% additive to the epoxy formulation returns a similar response (the scatter in the data reveal some higher values measured for modulus and strain, but there is a gradual reduction in the mechanical properties with increasing fortification thereafter (Fig. 7).

3.1.3. *Shear testing*

The results of the shear testing are shown in Table 3. The baseline specimens exhibit an average shear modulus of 0.92 ± 0.04 GPa. This is consistent with the manufacturer's datasheet value at around 1.0 GPa [21]. It is apparent that the addition of DMSO as a fortifier is more effective than DMC, presumably arising from the higher polarity of the former. All specimens containing DMSO displayed similar shear plots of shear stress *versus* shear strain (see Fig. S4) and a breakdown of one of the datasets (the composition containing 16 mol% DMSO) is shown in Fig. 8 as an example. The initial near linear region arises from the samples displaying elastic behaviour and this precedes a plastic region. The change in the gradient of the plot indicates that the sample undergoes strain hardening prior to failure. From these data, it is inferred

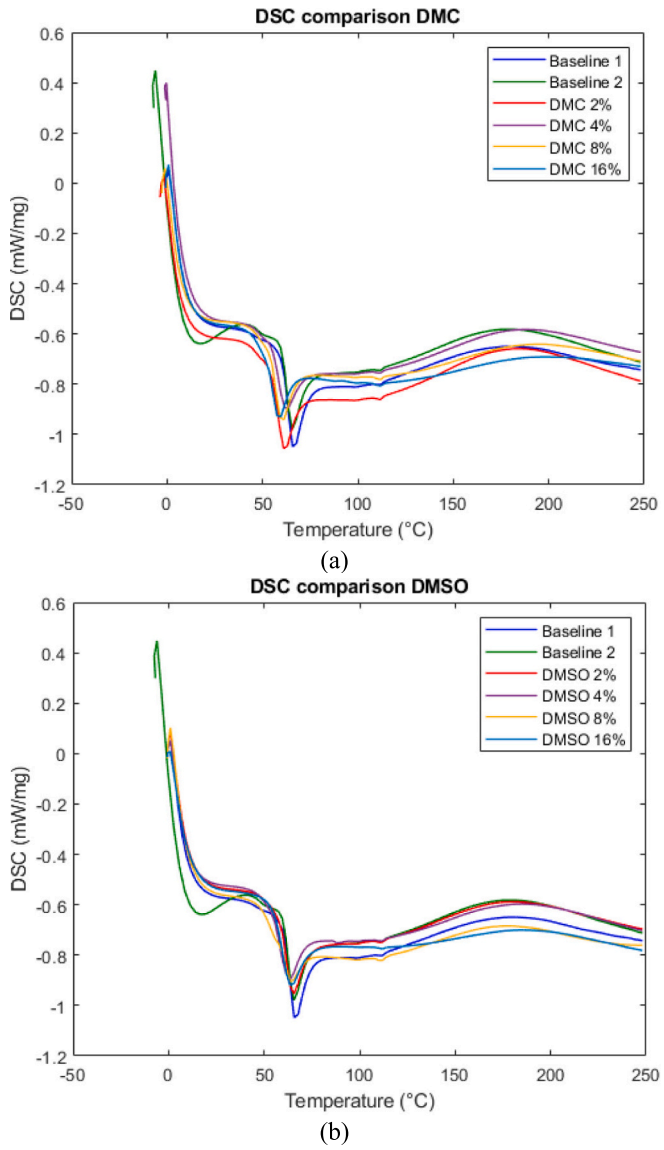

Fig. 5. DSC curves (exo upwards) for the uncured/partially cured blend of RS-M135, RS-MH137, containing (a) DMC (2–16 mol%) and (b) DMSO (2–16 mol %) when heated at 10 K/min under nitrogen. (N.B., Baseline 1 and Baseline 2 are baseline resin specimens).

Table 2
Compression data for the RS-M135/RS-MH137 epoxy following fortification with dimethyl carbonate (DMC) and dimethyl sulphoxide (DMSO) at different levels of addition (standard deviation shown in parentheses).

	Fortifier loading	Elastic modulus	Peak yield stress	Peak yield strain
	(mol%)	(GPa)	(MPa)	(S)
Baseline	0	3.16 (0.08)	−71.28 (1.48)	−0.032 (0.001)
DMC	2	3.55 (0.32)	−80.69 (1.34)	−0.033 (0.004)
	4	3.57 (0.64)	−78.73 (0.60)	−0.031 (0.003)
	8	3.13 (0.31)	−73.90 (1.57)	−0.034 (0.004)
	16	3.31 (0.28)	−72.90 (1.38)	−0.031 (0.004)
DMSO	2	3.52 (0.24)	−85.55 (0.95)	−0.035 (0.003)
	4	3.34 (0.23)	−85.53 (1.27)	−0.039 (0.003)
	8	3.08 (0.18)	−80.23 (1.07)	−0.042 (0.002)
	16	3.08 (0.13)	−80.95 (1.42)	−0.037 (0.003)

that the incorporation of DMSO can confer modest enhancements to the mechanical properties such as stiffness, strength and resistance to deformation, when measured in shear. The addition of DMSO was effective at all levels of addition improving all shear properties, *e.g.* with improvements of 16% increase in shear modulus, 15% in peak yield stress, and 13% in fracture shear stress following the addition of 4 mol% DMSO. The properties are enhanced at the highest loading but beyond 8 mol% the trend is in decline.

When the same epoxy was tested following incorporation of DMC (only specimens containing 2 and 4 mol% were tested), the samples generally displayed poorer mechanical performance across all parameters except peak yield stress and yield strain, compared with the unmodified RS-M135/RS-MH137 epoxy (see Table 3). Although similar shear plots of torque *versus* time were obtained, the precision became poorer as the DMC content was increased (Fig. S2) and the shear response of a representative specimen fortified with 4 mol% DMC, depicted in Fig. 9, has shown that there was no evidence of shear hardening. A gradual reduction in the mechanical properties with increasing DMC addition is observed (Fig. 10).

3.2. Thermal analysis of the uncured fortified blends

Initially, thermogravimetric analysis (TGA) was performed using the STA on the range of uncured epoxy systems fortified with DMSO to determine whether the fortifier would be lost during cure. The plot of mass loss *versus* temperature as a function of fortifier concentration is shown in Fig. 11. DMSO is hygroscopic and the mass loss at 100 °C is consistent with the evaporation of moisture (Fig. 11a), while the boiling point of DMSO is 189 °C [27] and this is indicated on the plot. A similar analysis was performed on the range of uncured epoxy systems fortified with DMC and the plot of mass loss *versus* temperature as a function of fortifier concentration is shown in Fig. 11b. The boiling point of DMC is 96 °C [28] and this is indicated on the plot. The observed bulk mass losses, attributed to water, reached only 4-5 wt% for the highest loadings (16 mol%) of the fortifiers. As the RS-M135/RS-MH137 epoxy system is degassed and cured at room temperature, the mass losses indicate that the fortifiers should remain in the blend during cure.

3.3. Thermal analysis of the cured fortified blends

Following cure, STA was performed on the epoxy systems fortified with both DMSO and DMC to determine whether the addition of the fortifier would result in a significant loss of thermal stability. The plot of mass loss *versus* temperature as a function of fortifier concentration is shown in Fig. 11. The degradation temperatures are quite similar between the two fortifiers (DMC degradation temperatures are comparable to or slightly lower than DMSO across different concentrations) and broadly comparable with the cured unmodified epoxy (Table 4).

The glass transition temperature (T_g) for the neat, cured epoxy samples which show the highest values (63 °C) recorded in the study (Table 4). Lesser et al. observed a similar effect on the T_g of fortified samples which were found to have superior mechanical properties [1]. However, a higher T_g can also affect the processing of the resin, which may require higher curing temperatures and/or longer curing times to achieve optimal properties. The cured, unfortified epoxy resin samples display the highest T_g values while the addition of all fortifiers leads to a modest drop in T_g, with the effect most marked with the addition DMSO. Nevertheless, the greatest reduction in T_g (of *ca.* 8 °C) was observed when 16 mol% DMC was added. Given that the results of the effects of DMSO and DMC on the glass transition temperature of epoxy resin show that these two additives reduce the glass transition temperature of epoxy resin, albeit more marginally in the case of the DMSO, this indicates that these two additives have the ability to promote the mobility of epoxy resin chain segments, *i.e.*, they may function as plasticizers.

3.4. Analysis of fortifier dispersion using molecular simulation

Although the first reports of the use of molecular simulation to model

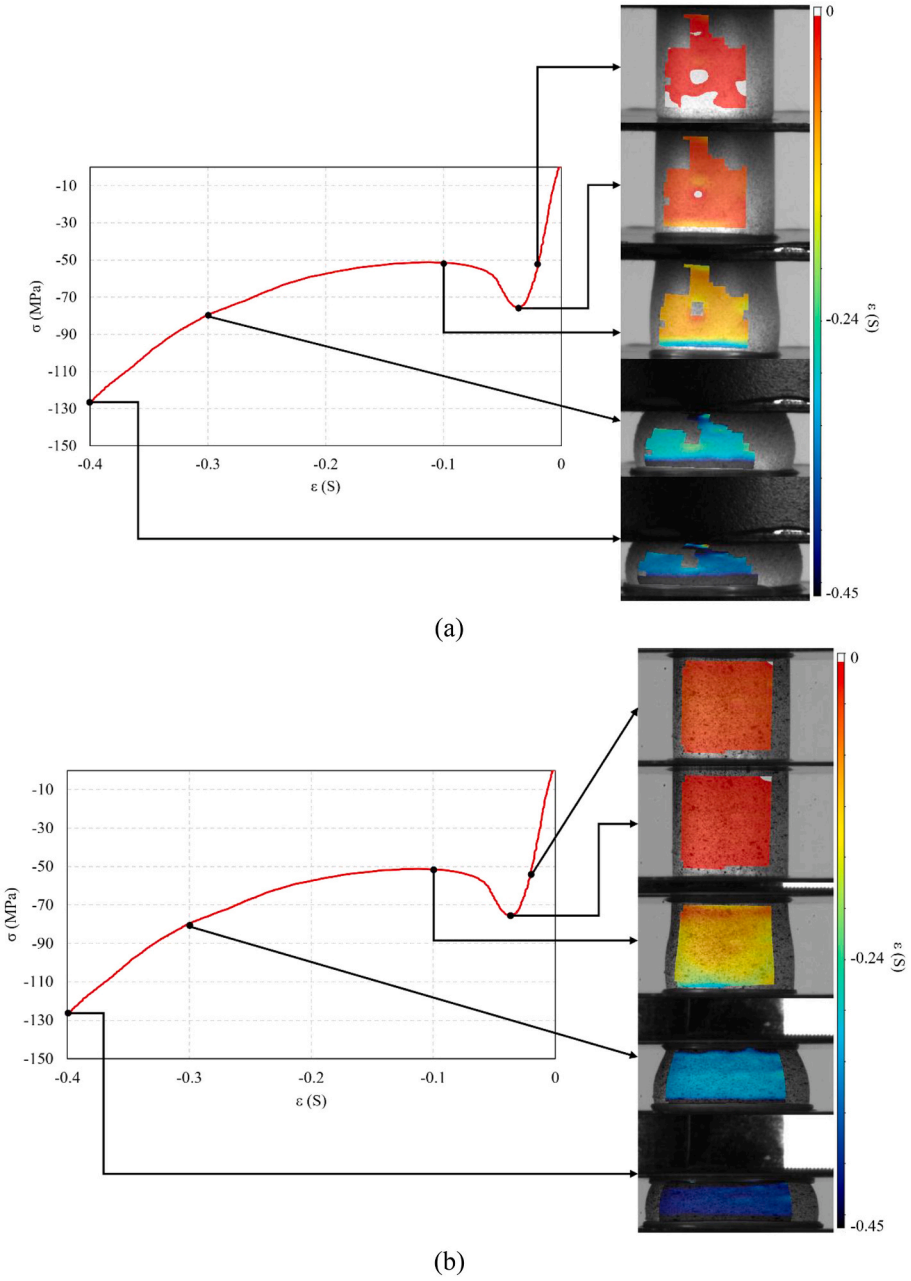

Fig. 6. The compressive stress-strain curves of the RS-M135/RS-MH137 epoxy fortified with (a) DMC (16 mol%) and (b) DMSO (16 mol%), with DIC images to show the compressive strain development in the gauge section.

the properties of thermosetting polymers is almost 30 years old now [29], it is now significantly more accepted within the materials community to visualise molecular architecture and predict physical and mechanical properties. In the present study, the unreacted monomers were modelled to explore the topology of the blend, provide an insight into the atomic interactions [30], and hence the miscibility of the components. There have been recent strategies, verified by molecular simulation, to utilise partially reacted substructures to develop a network topology to strain harden under tension while not significantly affecting the T_g, an issue facing the use of fortifiers [31]. Given that it is crucial to ensure that fortifiers used in the system are able to disperse as homogeneously as possible, avoiding the formation of aggregates of the fortifier, and ensuring efficient use of the fortifier. This factor was of key consideration in determining the ideal concentration of fortifier to be used.

In this study, MD was used to examine the topology of the fortifier in the epoxy blend, taking into account the epoxy resin's structural characteristics and the interactions with reinforcing agents, to understand the spatial arrangement of molecules and determine the dispersion of each fortifier in the liquid epoxy. Consequently, mixtures comprising RS-M135 and RS-MH137 at a range of loadings: 2 mol%, 4 mol%, 8 mol %, and 16 mol% to confirm the compatibility of the network with the fortifier.

In each case all molecules were considered and the close contacts (< 0.5 nm) between each were identified, from this summation, the proportion of molecules in close contact (expressed as a percentage of all possible available contacts) was determined and is shown below (Table 5). In this way, the proximity of each molecular fortifier to other molecular fortifier molecule can be gauged and the level of self-association predicted. This table (and those following) indicates the simulated topology of the uncured blend, *i.e.* the proximity of the monomer/curing agent/fortifier molecules in the mixture. Each row

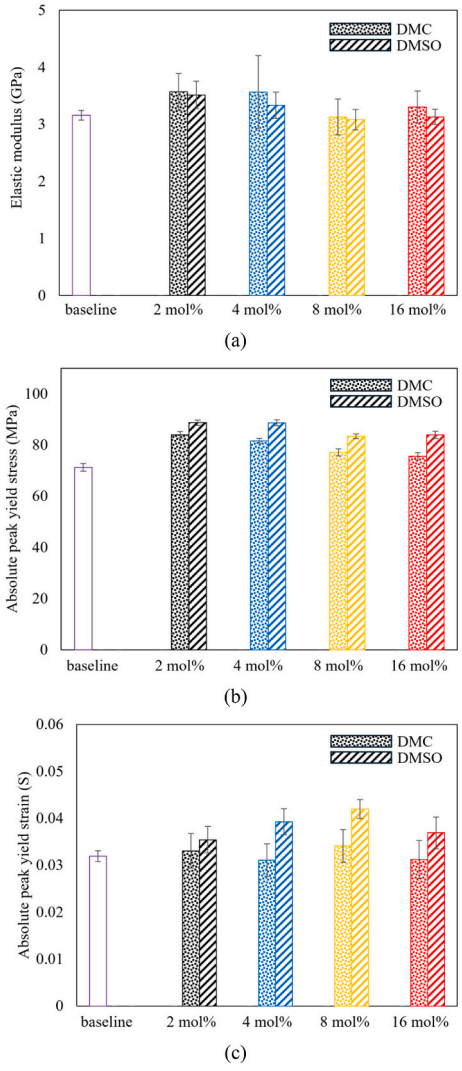

Fig. 7. Combined mechanical properties of (a) elastic modulus, (b) absolute peak yield stress, and (c) absolute peak yield strain measured in compression for the RS-M135/RS-MH137 epoxy (baseline) fortified with DMC (dot fill) and DMSO (strip fill). (Key: no pattern = baseline, black = 2 mol%, blue = 4 mol%, yellow = 8 mol%, red = 16 mol%). (For interpretation of the references to colour in this figure legend, the reader is referred to the web version of this article.)

Table 3
Shear properties for the RS-M135/RS-MH137 epoxy fortified with different concentrations of DMSO and DMC (standard deviation shown in parentheses).

	Fortifier loading	Shear modulus	Peak yield stress	Peak yield strain	Shear stress at fracture	Shear strain at fracture
	(mol%)	(GPa)	(MPa)	(S)	(MPa)	(S)
Baseline	0	0.92 (0.04)	44.43 (1.30)	0.08 (0.02)	51.3 (2.85)	1.00 (0.04)
DMC	2	0.89 (0.09)	46.11 (3.02)	0.11 (0.04)	41.0 (1.77)	0.80 (0.07)
	4	0.84 (0.14)	45.47 (5.42)	0.12 (0.02)	42.9 (6.43)	0.76 (0.13)
DMSO	4	1.07 (0.08)	51.12 (4.49)	0.09 (0.01)	57.9 (6.12)	1.20 (0.03)
	8	1.07 (0.08)	50.06 (2.14)	0.07 (0.02)	58.4 (7.64)	1.18 (0.05)
	16	1.02 (0.03)	45.48 (1.44)	0.07 (0.01)	49.1 (2.21)	1.12 (0.04)

shows the percentage of each type of molecule that is self-associated for each fortifier loading. Thus, if the number is large then it indicates that a large proportion of the molecules associate with themselves rather than another molecule; this provides a comparison of each blend. The grey highlight indicates the topological data for 'molecule 5' (which is the fortifier in each case).

This is also shown graphically in Fig. 12 for the simulated blend containing the liquid epoxy/curing agent blend and DMC. The latter typically exists as two conformers, a highly stable *cis–cis* conformer exhibiting a low dipole moment, generally reported to be around 0.91–0.93 D, and smaller amounts of a *cis–trans* conformer possessing a much higher dipole moment of approximately 4.5 D [32]. Initially, it is difficult to observe the degree of self-association due to the packed unit cell (Fig. 13a) and variety of atoms in the blend. However, once the epoxy components have been removed from the unit cell (Fig. 13b) the proximity of the remaining DMC molecules is clear. Even at the highest concentration used, agglomeration of the fortifier is limited. A similar simulation was performed using the DMSO fortifier (which has a dipole moment of 3.96–4.1 D) and the topology of the uncured blend containing DMSO shows a stronger association with the epoxy network (Table 6). However, when the image of the uncured, fortified blend containing 16 mol% DMSO is examined (Fig. 14) then the simulated data reveal that there is still very little of self-association even at the highest concentration. Examination of the simulation data in Table 5 for DMC (*i.e.* the shaded grey area) indicate that self-association is comparatively low (25–26%) at 2–4 mol%, but begins to rise (exceeding 30–36%) as the loading increases to 8–16 mol%. DMSO (Table 6) displays a similar level of self-association at the lowest loading (*ca.* 25% at 2 mol%, 26–27% at 4 mol%), but once again this rises to a similar level (*ca.* 30% at 8 mol%) and is even higher than DMC (40% at 16 mol%). There is some variation in the predicted values for Molecules 2 and 3 at lower concentrations. As the simulations were run in duplicate for each combination, it is assumed that the disparity arises from the limited number of simulations performed and the limited size of the data set (*i.e.* that the difference would have been smaller had more simulations been carried out on larger simulation sets).

The selection of the molecular fortifiers for this study had been driven by the reported success of the use of DMMP, which at additions of 15–20 mol% was reported [1] to increase the T_g of the unmodified epoxy by up to 15–20 °C and the tensile strength by *ca.* 20 MPa. However, the substitution of BHPPO for DMMP proved problematic in use. While the DMSO and DMC proved easy to disperse, even at relatively high concentrations, the BHPPO tended to agglomerate and showed very strong self-association at higher concentrations in this epoxy network (Table 7), leading to real difficulty in making up a fortified blend. No dipole moment could be identified for BHPPO but for triphenylphosphine oxide, which also contains the same central bridge, a figure of 4.44 D is accepted [33].

For the simulated blend containing the liquid epoxy/curing agent blend and BHPPO (Fig. 15), it was initially difficult to observe the self-association due to the packed unit cell and variety of atoms in the blend. However, once the epoxy component had been removed from the unit cell the proximity of the remaining BHPPO molecules was clear, particularly in the lower right region of the model. This is distinctly different from the previous models with DMC and DMSO which show even at high concentration a relatively even distribution in between the epoxy network. The marked contrast with BHPPO compared with DMC and DMSO is evident immediately. It was observed in the modelling experiment that in the case of BHPPO, the topology figure is consistently high, regardless of BHPPO loading (and a self-association of between 47.9 and 49.1% when a concentration of 16% concentration of the fortifier was simulated), suggesting that almost half of the BHPPO molecules prefer to associate with another BHPPO molecule rather than an epoxy or diamine; compare this with *e.g.* DMC in which the figure is *ca.* 20–30%, thus verifying the experimental observations.

A further phosphate fortifier (9,10-dihydro-9-oxa-10-

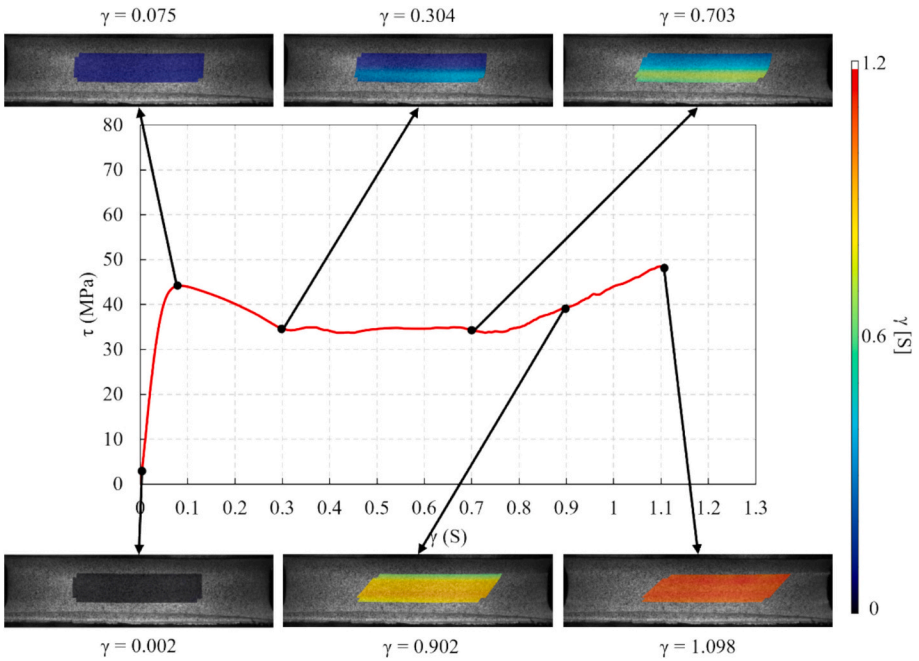

Fig. 8. The shear stress-strain curve of a RS-M135/RS-MH137 epoxy fortified with DMSO (16 mol%), with DIC images to show the shear strain development in the gauge section.

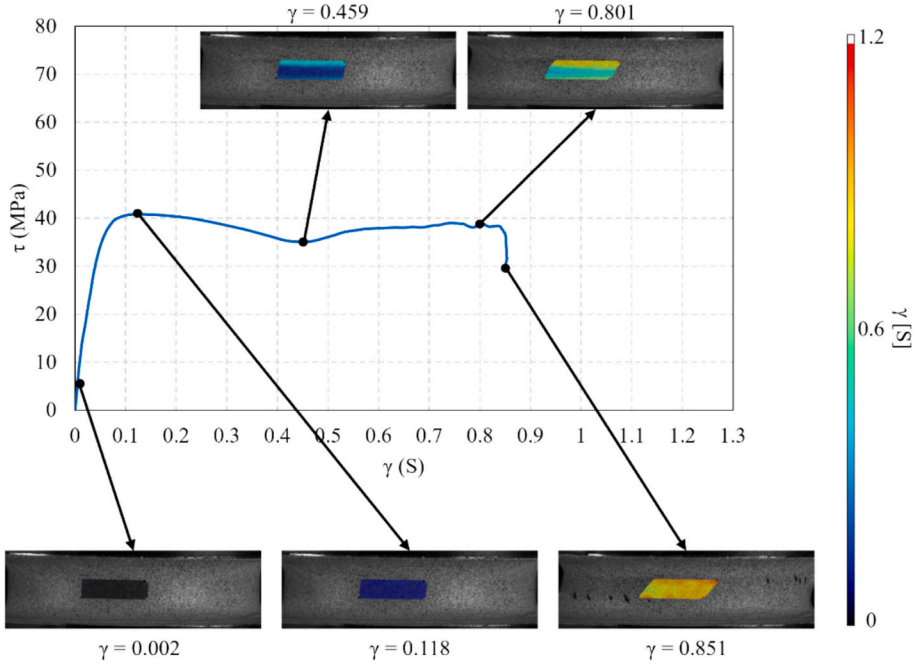

Fig. 9. The shear stress-strain curve of a RS-M135/RS-MH137 epoxy fortified with DMC (4 mol%), with DIC images to show the shear strain development in the gauge section.

phosphaphenanthrene-10-oxide, DOPO) was considered, but this was simulated before performing any experimental work. However, in common with BHPPO, DOPO displayed a strong degree of self-association in the simulation (43% at 16% concentration of DOPO, see Table S1 and Fig. S5 in Supplementary Material) and this result was verified *via* preliminary laboratory blending experiments, so this was not progressed in depth empirically. In summary, both DMC and DMSO (both significantly smaller molecules, polar, traditional organic solvents and capable of hydrogen bonding with the hydroxyl moieties of the epoxy dimer) were more prone to associate with the epoxy, while BHPPO/DOPO (both significantly larger, rigid aromatic phosphorous-containing structures) displayed significantly more evident self-association behaviour.

4. Conclusions

This study has shown that there is benefit in using relatively low concentrations of molecular fortifiers to improve the compression properties of crosslinked networks. The use of DMSO as a molecular fortifier in this study has shown a modest increase in compression (11%

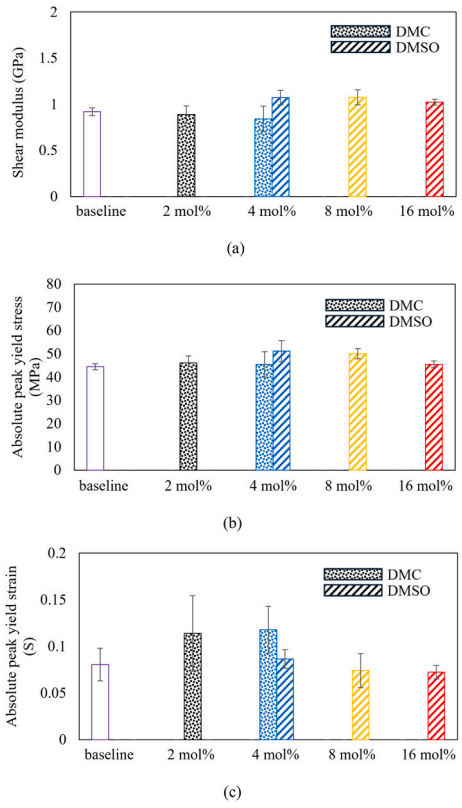

Fig. 10. Combined mechanical properties of (a) shear modulus, (b) absolute peak yield stress, and (c) absolute peak yield strain measured in shear for the RS-M135/RS-MH137 epoxy (baseline) fortified with DMC (dot fill) and DMSO (strip fill). (Key: no pattern = baseline, black = 2 mol%, blue = 4 mol%, yellow = 8 mol%, red = 16 mol%). (For interpretation of the references to colour in this figure legend, the reader is referred to the web version of this article.)

increase in compression modulus; 24% in peak yield stress; 11% in peak yield strain, with 2 mol% DMSO) and shear properties (16% increase in shear modulus; 15% in peak yield stress; 12.5% in peak yield strain, with 4 mol% DMSO) when compared with the unmodified commercial infusion epoxy matrix. The impact on T_g was minimal but did serve to reduce the temperature recorded by (3 °C). The improvements in compression observed in this work compare favourably with the 20% increase in tensile modulus reported by Lesser et al. for the network formed from the diglycidyl ether of bisphenol-A (Epon 825), dimethyl ethylenediamine, and ethylene diamine, when fortified with 15 mol% DMMP, albeit using a more readily available less polar fortifier.

From the literature cited, organophosphorus compounds appeared to be the most promising candidates for study as fortifiers, but that the specific molecule used in the seminal study (DMMP, a known nerve agent mimic) would present sufficiently large challenges in manufacturing steps to render it impractical in use. Consequently, other less harmful commercial organophosphorus compounds (flame retardants) were considered instead. Unfortunately, when initial laboratory trials were performed with the DOPO, similar results to the BHPPO were observed and it was decided not to proceed further to a full study but simply to perform the simulation. Therefore, while it was decided not to further investigate this material, it was felt that this should be mentioned in the manuscript for the guidance of future researchers.

During the refereeing of this manuscript, a referee raised the pertinent question of technological applicability/scale, and this has not really addressed this aspect in the manuscript. In short, if the fortifier were (a) to be one of those indicated or similar DMSO, DMC – both readily commercially available and REACH compliant), (b) to be used at the loadings identified (which are modest), and (c) intended for use as a

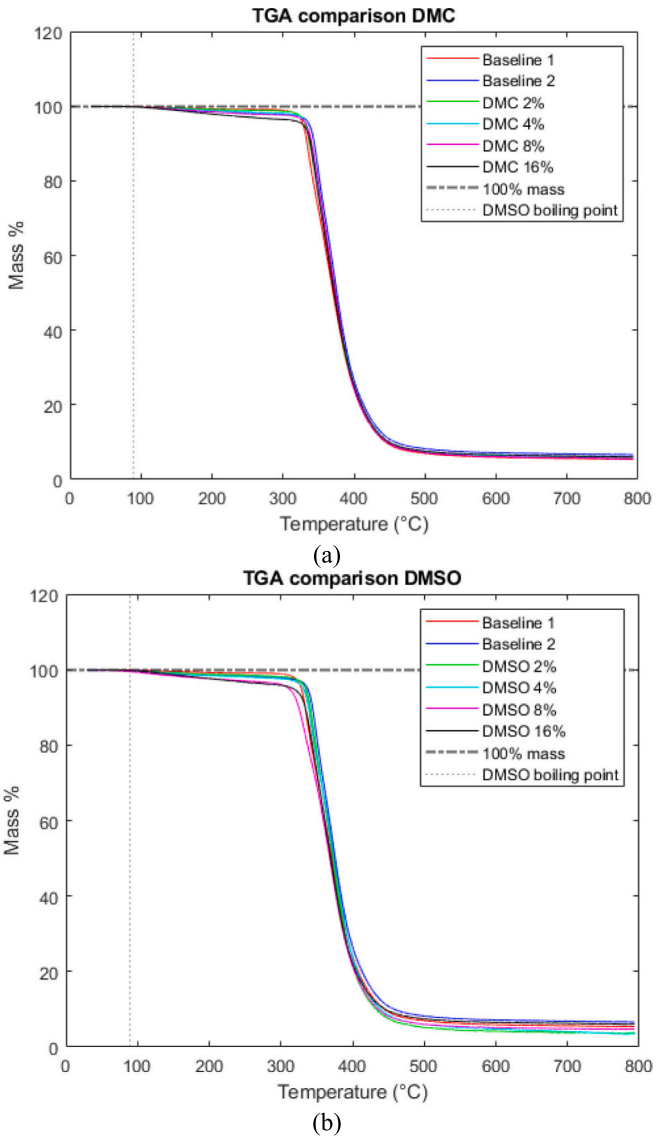

Fig. 11. Plot of mass loss *versus* temperature for the uncured blend of RS-M135, RS-MH137, and (a) DMC (2–16 mol%) and (b) DMSO (2–16 mol%) when heated at 10 K/min under nitrogen. (*N.B.*, Baseline 1 and Baseline 2 are baseline resin specimens).

Table 4
Selected thermal properties of cured RS-M135/RS-MH137 epoxy as a function of molecular fortifier content.

Fortifier	Concentration (mol%)	T_g (°C)[1]	Degradation temperature (°C)[2]
Baseline	0	63	327
Baseline	0	63	339
DMSO	2	62	336
DMSO	4	59	333
DMSO	8	60	318
DMSO	16	60	330
DMC	2	58	330
DMC	4	59	333
DMC	8	57	335
DMC	16	55	335

[1] T_g was measured using DSC.
[2] degradation temperature = temperature at which ($T_{5\%}$) mass loss was recorded.

fluid blend in an infusion process, such as RTM (rather than laid up using prepreg) then it could be scaled industrially. However, further study

Table 5
Simulated topology data for the dispersion of the epoxy containing DMC.*

Fortifier concentration (mol%)	Molecule*	Topology (%)	Topology (%)
2	1	55.4%	47.3%
	2	1.8%	5.5%
	3	14.4%	7.5%
	4	3.6%	14.4%
	5	24.7%	25.3%
4	1	49.6%	49.7%
	2	4.2%	4.3%
	3	10.9%	9.6%
	4	8.3%	10.5%
	5	27.0%	26.0%
8	1	47.4%	44.9%
	2	3.5%	5.5%
	3	10.9%	10.6%
	4	6.7%	9.6%
	5	31.5%	29.3%
16	1	48.7%	43.3%
	2	4.4%	5.1%
	3	8.1%	9.0%
	4	6.2%	6.8%
	5	32.5%	35.8%

* Key: molecule 1 = DGEBA, molecule 2 = DEGH, molecule 3 = 3-aminomethyl-3,5,5-trimethylcyclohexylamine, molecule 4 = polyoxypropylenediamine, and molecule 5 = DMC. *N.B.*, the grey cells indicate the simulated proximity data for the fortifier.

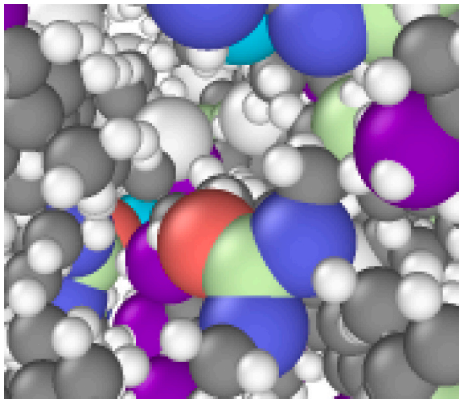

Fig. 12. Molecular simulation showing close packed section of unit cell comprising the baseline epoxy containing 16 mol% DMC molecules (DMC molecule shown at centre of image). (Key: white = hydrogen atoms, black = sp^3 carbon atoms, red = sp^2 oxygen atoms, olive = sulphur atoms, blue = sp^3 oxygen atoms, purple = nitrogen atoms). (For interpretation of the references to colour in this figure legend, the reader is referred to the web version of this article.)

would be necessary to determine (a) the extent of shelf life in the non-reactive component of the blend (*i.e.* to determine when the fortifier would need to be introduced at time of delivery to the mould, (b) whether any settling occurs on storage. None of these aspects were considered in this fundamental study.

Although the range of commercially available phosphates, with acceptable toxicity, is somewhat limited, molecular modelling demonstrated the propensity of BHPPO and DOPO to undergo self-association when in the presence of the epoxy making dispersion very difficult to achieve during polymerisation, negating their use as molecular fortifiers. The use of simulation for the purpose of selecting molecular fortifiers for their suitability for dispersion in an epoxy network may enable users to make pre-informed decisions on the additives saving time and costs as valuable resources.

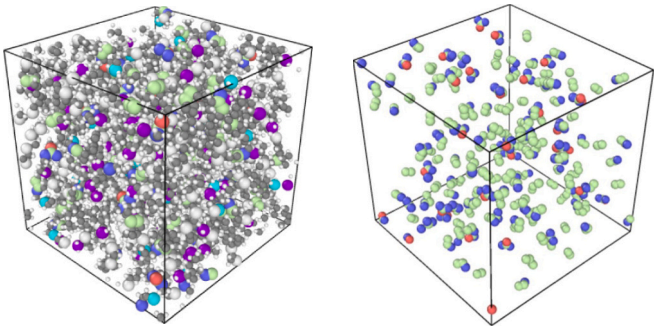

Fig. 13. Molecular simulation showing unit cell comprising 16 mol% DMC molecules (*N.B.*, epoxy matrix omitted from diagram on the right). Key: olive = sulphur atoms, purple = oxygen atoms. (For interpretation of the references to colour in this figure legend, the reader is referred to the web version of this article.)

Table 6
Simulated topology data for the dispersion of the epoxy containing DMSO.*

Fortifier concentration (mol%)	Molecule*	Topology (%)	Topology (%)
2	1	53.7%	50.3%
	2	9.5%	5.2%
	3	4.7%	11.8%
	4	7.8%	8.0%
	5	24.3%	24.7%
4	1	43.7%	47.7%
	2	10.1%	7.7%
	3	8.5%	11.8%
	4	10.5%	6.3%
	5	27.3%	26.5%
8	1	47.5%	46.2%
	2	3.5%	5.5%
	3	11.1%	8.4%
	4	9.2%	8.9%
	5	28.7%	31.0%
16	1	43.7%	42.8%
	2	3.7%	4.8%
	3	7.9%	8.1%
	4	4.8%	6.0%
	5	39.9%	38.3%

* Key: molecule 1 = DGEBA, molecule 2 = DEGH, molecule 3 = 3-aminomethyl-3,5,5-trimethylcyclohexylamine, molecule 4 = polyoxypropylenediamine, and molecule 5 = DMSO. *N.B.*, the grey cells indicate the simulated proximity data for the fortifier.

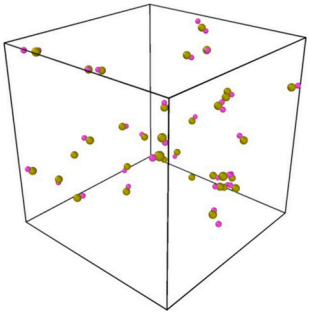

Fig. 14. Molecular simulation showing unit cell comprising 16 mol% DMSO molecules (*N.B.*, epoxy matrix and methyl residues omitted from the diagram). Key: olive = sulphur atoms, purple = oxygen atoms. (For interpretation of the references to colour in this figure legend, the reader is referred to the web version of this article.)

Table 7
Simulated topology data for the dispersion of the epoxy containing BHPPO.*

Fortifier concentration (mol%)	Molecule*	Topology (%)	Topology (%)
2	1	34.5	32.1
	2	4.5	10.0
	3	8.5	9.6
	4	6.3	6.2
	5	46.1	42.1
4	1	28.9	27.8
	2	13.3	10.3
	3	9.1	7.1
	4	7.2	10.2
	5	41.6	44.5
8	1	33.8	32.2
	2	6.3	8.5
	3	10.9	10.4
	4	5.6	5.4
	5	43.4	43.5
16	1	27.9	27.7
	2	9.1	8.3
	3	10.1	8.2
	4	5.2	6.7
	5	47.7	49.1

* Key: molecule 1 = DGEBA, molecule 2 = DEGH, molecule 3 = 3-aminomethyl-3,5,5-trimethylcyclohexylamine, molecule 4 = polyoxypropylenediamine, and molecule 5 = BHPPO. *N.B.*, the grey cells indicate the simulated proximity data for the fortifier.

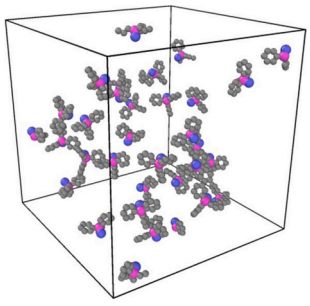

Fig. 15. Molecular simulation showing unit cell comprising the BHPPO molecules (*N.B.*, epoxy matrix and hydroxyl groups hidden in the diagram). Key: black = sp^2 carbon atoms, blue = sp^2 oxygen atoms, purple = phosphorus atoms. (For interpretation of the references to colour in this figure legend, the reader is referred to the web version of this article.)

CRediT authorship contribution statement

Bohao Zhang: Writing – review & editing, Visualization, Methodology, Investigation, Formal analysis. **Rachel Board:** Writing – review & editing, Visualization, Investigation. **Eleni Georgiou:** Writing – review & editing, Investigation, Formal analysis. **Laurie-Anne Entzmann:** Writing – review & editing, Investigation, Formal analysis. **Joe Rifai:** Writing – review & editing, Investigation, Formal analysis. **Nicolas S.T. Darras:** Writing – review & editing, Investigation, Formal analysis. **Matthew Bone:** Writing – review & editing, Visualization, Software. **Gustavo Quino:** Writing – review & editing, Supervision, Formal analysis. **Milo S.P. Shaffer:** Writing – review & editing, Supervision, Project administration, Funding acquisition. **Ian Hamerton:** Writing – original draft, Supervision, Funding acquisition, Conceptualization.

Declaration of competing interest

The authors declare the following financial interests/personal relationships which may be considered as potential competing interests:

Eleni Georgiou reports financial support was provided by Engineering and Physical Sciences Research Council. Joe Rifai reports financial support was provided by Engineering and Physical Sciences Research Council. Nicolas ST Darras reports financial support was provided by Engineering and Physical Sciences Research Council. Matthew Bone reports financial support was provided by Engineering and Physical Sciences Research Council. Laurie-Anne Entzmann reports financial support was provided by Engineering and Physical Sciences Research Council. If there are other authors, they declare that they have no known competing financial interests or personal relationships that could have appeared to influence the work reported in this paper.

Acknowledgements

The authors would like to acknowledge funding which supported this work from the UK Research and Innovation - EPSRC Programme Grant; Next Generation Fibre-Reinforced Composites: A Full Scale Redesign for Compression (EP/T011653/1), a collaboration between the University of Bristol and Imperial College London, UK. JG, EG, and MB are supported by the Engineering and Physical Science Research Council as part of the EPSRC Centre for Doctoral Training in Composites Science, Engineering, and Manufacturing. Grant number: EP/S021728/1.

For the purpose of open access, the author has applied a Creative Commons Attribution (CC BY) licence to any Author Accepted Manuscript version arising.

Appendix A. Supplementary data

Supplementary data to this article can be found online at https://doi.org/10.1016/j.reactfunctpolym.2026.106827.

Data availability

Data will be made available on request.

References

[1] A.J. Lesser, K. Calzia, M. Junk, Reinforcement of epoxy networks with sulfur-and carbon-based molecular fortifiers, Polym. Eng. Sci. 47 (10) (2007) 1569–1575, https://doi.org/10.1002/pen.20862.
[2] S.M. Seraji, H. Gan, N.D. Le, J. Zhang, R.J. Varley, The effect of DOPO concentration and epoxy amine stoichiometry on the rheological, thermal, mechanical and fire-retardant properties of crosslinked networks, Polym. Int. 71 (11) (2022) 1320–1329, https://doi.org/10.1002/pi.6436.
[3] C.F. Kins, G. Brunklaus, H.W. Spiess, New phosphonate-based additives for fortification in model epoxies, Macromolecules 46 (6) (2013) 2067–2077, https://doi.org/10.1021/ma400093w.
[4] C. Saraf, E. Stubbs, W. Hu, T. Emrick, A.J. Lesser, Combining mechanical fortification and ultralow flammability in epoxy networks, Macromol. Mater. Eng. 306 (2) (2021) 2000567, https://doi.org/10.1002/mame.202000567.
[5] K.J. Calzia, A. Forcum, A.J. Lesser, Comparing reinforcement strategies for epoxy networks using reactive and non-reactive fortifiers, J. Appl. Polym. Sci. 102 (5) (2006) 4606–4615, https://doi.org/10.1002/app.24401.
[6] K. Utaloff, M.H. Kothmann, M. Ciesielski, M. Döring, T. Neumeyer, V. Altstädt, I. Gorman, M. Henningsen, Improvement of fracture toughness and glass transition temperature of DGEBA-based epoxy systems using toughening and crosslinking modifiers, Polym. Eng. Sci. 59 (1) (2019) 86–95, https://doi.org/10.1002/pen.24870.
[7] W. Jackson Jr., J. Caldwell, Antiplasticization. III. Characteristics and properties of antiplasticizable polymers, J. Appl. Polym. Sci. 11 (2) (1967) 227–244, https://doi.org/10.1002/app.1967.070110206.
[8] A. Garton, P.D. McLean, W.T. Stevenson, J.N. Clark, J.H. Daly, Additives for improving the strength, stiffness, and ductility of epoxy resins, Polym. Eng. Sci. 27 (21) (1987) 1620–1626, https://doi.org/10.1002/pen.760272108.
[9] J. Daly, A. Britten, A. Garton, P. McLean, An additive for increasing the strength and modulus of amine-cured epoxy resins, J. Appl. Polym. Sci. 29 (4) (1984) 1403–1414, https://doi.org/10.1002/app.1984.070290433.
[10] L. Heux, F. Lauprêtre, J. Halary, L. Monnerie, Dynamic mechanical and 13C nmr analyses of the effects of antiplasticization on the β secondary relaxation of aryl-aliphatic epoxy resins, Polymer 39 (6–7) (1998) 1269–1278, https://doi.org/10.1016/S0032-3861(97)00423-0.
[11] S.R. Swan, H. Gan, C. Creighton, J.M. Griffin, B.V. Gashi, R.J. Varley, Improving mechanical properties and processability of a very high Tg epoxy amine network via anti-plasticizer fortification, J. Appl. Polym. Sci. 139 (36) (2022) e52854, https://doi.org/10.1002/app.52854.
[12] M. Abraham, I. Hamerton, J. Rose, J. Grate, Hydrogen bonding. Part 18. Gas–liquid chromatographic measurements for the design and selection of some hydrogen bond acidic phases suitable for use as coatings on piezoelectric sorption detectors,

J. Chem. Soc. Perkin Trans. 2 (9) (1991) 1417–1423, https://doi.org/10.1039/P29910001417.
[13] G. Quino, J. Gargiuli, S. Pimenta, I. Hamerton, P. Robinson, R.S. Trask, Experimental characterisation of the dilation angle of polymers, Polym. Test. 125 (2023) 108137, https://doi.org/10.1016/j.polymertesting.2023.108137.
[14] Y. Xu, G. Quino, K.R. Ramakrishnan, A. Pellegrino, Effects of build orientation and strain rate on the tensile-shear behaviour of polyamide-12 manufactured via laser powder bed fusion, Mater. Des. 232 (2023) 112162, https://doi.org/10.1016/j.matdes.2023.112162.
[15] ASTM D695–23, Standard Test Method for Compressive Properties of Rigid Plastics, ASTM, 2023.
[16] S.L. Mayo, B.D. Olafson, W.A. Goddard, DREIDING: a generic force field for molecular simulations, J. Phys. Chem. 94 (26) (1990) 8897–8909, https://doi.org/10.1021/j100389a010.
[17] E. Paquet, H.L. Viktor, Molecular dynamics, Monte Carlo simulations, and langevin dynamics: a computational review, Biomed. Res. Int. 2015 (1) (2015) 183918, https://doi.org/10.1155/2015/183918.
[18] M.-S. Li, C.-C.M. Ma, M.-L. Lin, F.-C. Chang, Chemical reactions occurring during the preparation of polycarbonate-epoxy blends, Polymer 38 (19) (1997) 4903–4913.
[19] P. Worsawat, P. Noppawan, C. Croise, N. Supanchaiyamat, C.R. McElroy, A. J. Hunt, Acid-catalysed reactions of amines with dimethyl carbonate, Org. Biomol. Chem. 21 (2023) 1070–1081.
[20] S. Antoniotti, S. Antonczak, J. Golebiowski, Acid-catalysed oxidative ring-opening of epoxide by DMSO. Theoretical investigation of the effect of acid catalysts and substituents, Theor. Chem. Accounts 112 (4) (2004) 290–297.
[21] Ultra Low Viscosity Epoxy System RS-M135 Hardeners RS-MH134 & RS-MH137 for RTM & Vacuum Infusion Processes. www.prfcomposites.com, 2026.
[22] X. Morelle, J. Chevalier, C. Bailly, T. Pardoen, F. Lani, Mechanical characterization and modeling of the deformation and failure of the highly crosslinked RTM6 epoxy resin, Mech. Time-Depend. Mater. 21 (2017) 419–454, https://doi.org/10.1007/s11043-016-9336-6.
[23] G. Quino, A. Pellegrino, V.L. Tagarielli, N. Petrinic, Measurements of the effects of pure and salt water absorption on the rate-dependent response of an epoxy matrix, Compos. B Eng. 146 (2018) 213–221, https://doi.org/10.1016/j.compositesb.2018.03.044.
[24] E.M. Arruda, M.C. Boyce, Evolution of plastic anisotropy in amorphous polymers during finite straining, Int. J. Plast. 9 (6) (1993) 697–720, https://doi.org/10.1016/0749-6419(93)90034-N.
[25] M. Boyce, E. Arruda, An experimental and anaiytical investigation of the large strain compressive and tensile response of glassy polymers, Polym. Eng. Sci. 30 (20) (1990) 1288–1298, https://doi.org/10.1002/pen.760302005.
[26] R.N. Haward, G. Thackray, The use of a mathematical model to describe isothermal stress-strain curves in glassy thermoplastics, Proc. R. Soc. Lond. Ser. A Math. Phys. Sci. 302 (1471) (1968) 453–472, https://doi.org/10.1098/rspa.1968.0029.
[27] Sigma Product Data Sheet for DMSO. https://www.sigmaaldrich.com/deepweb/assets/sigmaaldrich/product/documents/712/921/d8418pis.pdf, 2024 (28th March 2024).
[28] 616-38-6 (Dimethyl Carbonate) Product Description. https://www.chemicalbook.com/ChemicalProductProperty_US_CB8853983.aspx, 2024 (28th March 2024).
[29] I. Hamerton, C.R. Heald, B.J. Howlin, Molecular modelling of the physical and mechanical properties of two polycyanurate network polymers, J. Mater. Chem. 6 (3) (1996) 311–314, https://doi.org/10.1039/JM9960600311.
[30] G.M. Odegard, S.U. Patil, P.P. Deshpande, K. Kanhaiya, J.J. Winetrout, H. Heinz, S. P. Shah, M. Maiaru, Molecular dynamics modeling of epoxy resins using the reactive interface force field, Macromolecules 54 (21) (2021) 9815–9824, https://doi.org/10.1021/acs.macromol.1c01813.
[31] O. Aluko, S. Gotham, G. Odegard, A molecular dynamic modelling of cross-linked epoxy resin using reactive force field: thermo-mechanical properties, J. Mech. Eng. Autom. 5 (2015) 655–666, https://doi.org/10.17265/2159-5275/2015.12.002.
[32] S.K. Reddy, S. Balasubramanian, Liquid dimethyl carbonate: a quantum chemical and molecular dynamics study, J. Phys. Chem. B 116 (51) (2012) 14892–14902.
[33] Triphenylphosphine Oxide and Isomers. https://www.stenutz.eu/chem/solv6.php?name=triphenylphosphine+oxide#google_vignette, 2026 (accessed 18/04/26).